# Calibration and Demonstration of the New Virginia Tech Anechoic Wind Tunnel

Marcel C. Remillieux,[1] Erin D. Crede,[2] Hugo E. Camargo,[3]
Ricardo A. Burdisso,[4] William J. Devenport.[5]
Matthew Rasnick,[6] Philip Van Seeters[7], and Amanda Chou[8]
*Virginia Polytechnic Institute and State University, Blacksburg, VA, 24061*

**A unique new removable anechoic system and new acoustic treatment for the Virginia Tech Stability Wind Tunnel is described. The new system consists of a Kevlar-walled acoustic test section flanked by two anechoic chambers. In its new configuration the facility is closed aerodynamically and open acoustically, allowing far-field acoustic measurements with a flow quality comparable to that of a hard-walled wind tunnel. An extensive program of experiments has been conducted to examine the performance of this new hardware under a range of conditions, both to examine the effects of acoustic treatment on overall test-section noise levels and to ascertain the aerodynamic characteristics of the new test section. Noise levels in the test section of the anechoic facility are down by as much as 25 dB compared to the original hard-walled configuration. Lift interference corrections (for a baseline NACA 0012 airfoil) are less than half those expected in an open-jet wind tunnel. Acoustic measurements of airfoil trailing edge noise using a microphone phased array are compared to past experiments conducted on similar airfoils in an open-jet facility.**

## I. Introduction

EARLY research in aeroacoustics was exclusively conducted in open-jet wind tunnels. These facilities usually allow noise measurements to be carried out in the far field and in an anechoic environment. Open-jet wind tunnels, however, have two problems, both of which result from the free jet boundary. First, the jet shear layer formed at the boundary develops large eddies that entrain air from around the wind tunnel. At the point where the jet re-enters the tunnel, this leads to a source of instability and noise, both because of the eddies, and because the extra mass flow they contain cannot be reabsorbed into the wind tunnel circuit. The development of a quiet jet catcher can help, but this is possibly the most difficult and uncertain aspect of anechoic tunnel design. The second problem is that open-jet test sections are notoriously sensitive to lift interference. Interference occurs because a lifting model alters the path of the jet, changing the flow pattern from that which would be encountered in free flight. Lift interference can be a complicating factor in studies of acoustic emissions from aerodynamic surfaces under load.

The advent of microphone phased arrays in the early 1990s has rendered possible, and even common, the ability to collect acoustic data in hard-walled wind tunnels. Issues related to testing in hard-walled wind tunnels include, the size of the test section that sometimes does not allow acoustic measurements to be carried out in the far-field, background noise and reflections, and self-noise from the microphones exposed to the flow. Jaeger et al.[1] investigated different means of shielding a microphone phased array embedded in a wall of a test section. They found that tensioned thin weave Kevlar 120® (7.9 grams/cm2) transmitted

---

sound with very little attenuation up to at least 25 kHz, and to be much more durable than metal weave or fiberglass. They then compared measurements made with their phased array system recessed behind a Kevlar sheet and flush with the wind tunnel wall, demonstrating much greater signal-to-noise ratio in the former case. Tests with this material at Virginia Tech have produced similar results (Ravetta, et al.[2]).

Over the past few years, several modifications have been made to allow the current aerodynamic configuration to function as an anechoic facility; these modifications include the design of two anechoic chambers and a removable test section. In 2005, a prototype section was designed and tested[3,4] to validate the concept. These measurements included acoustic spectra of various tunnel treatment options, and aerodynamic measurements of a NACA 0012 airfoil section. Results of those measurements show the feasibility of creating an aerodynamically-closed and acoustically-open anechoic test section tunnel that will achieve better aerodynamic performance than a free jet facility, while maintaining comparable acoustic performance. In 2006 and 2007, a full scale version of the anechoic test section system was fabricated and installed in the VT Stability Wind Tunnel. An iterative sequence of calibration measurements and improvements were then performed, resulting in a facility that combines low background noise and high aerodynamic quality. The novel anechoic test section design utilizes Kevlar cloth to provide a stable flow boundary, which eliminates the need for a jet catcher and greatly reduces aerodynamic interference corrections. An extensive program of experiments has been conducted to examine the performance of this new hardware under a range of conditions.

This paper provides a description of this new facility and details of its optimization, calibration, and final characteristics. The paper also includes examples of acoustic measurements made in the facility over a range of configurations. The paper is organized as follows. Section II describes the VT Stability Wind Tunnel and the modifications to convert it to an anechoic facility. This includes descriptions of the anechoic test section and the noise treatment of the fan and tunnel circuit. Section III reports results on the aerodynamic and aeroacoustic performance of the tunnel in its original hard-walled configuration, the characteristics of the flow through the new anechoic test section in its initial configuration, the noise reduction due to the acoustic treatment in the tunnel circuit, and improvements in the anechoic test section. Section IV reports results on the aerodynamic and aeroacoustic characteristics of NACA 0012 airfoils, measured in this new facility. Spectra levels are compared with past experiments conducted in an open-jet wind tunnel by Brooks et al.[5]

## II.  Description of the Wind Tunnel

### A.  Facility Overview

The Stability Wind Tunnel at Virginia Tech is a continuous, single return, subsonic wind tunnel with 7.3-m long removable rectangular test sections of square cross section 1.83 m on edge. The general layout is illustrated in Figure 1.

The tunnel is powered by a 0.45-MW variable speed DC motor driving a 4.3-m propeller at up to 600 RPM. This provides a maximum speed in the test section (with no blockage) of about 75 m/s and a Reynolds number per meter of up to about 5,000,000. The tunnel forms a closed loop, but has an air exchange tower open to the atmosphere to allow for temperature stabilization. The air exchange tower is located downstream of the fan and motor assemblies. Downstream of the tower, the flow is directed into a 5.5×5.5-m settling chamber containing seven turbulence-reducing screens, each with an open area ratio of 0.6 and separated by 0.15 m. Flow exits this chamber through the 9:1
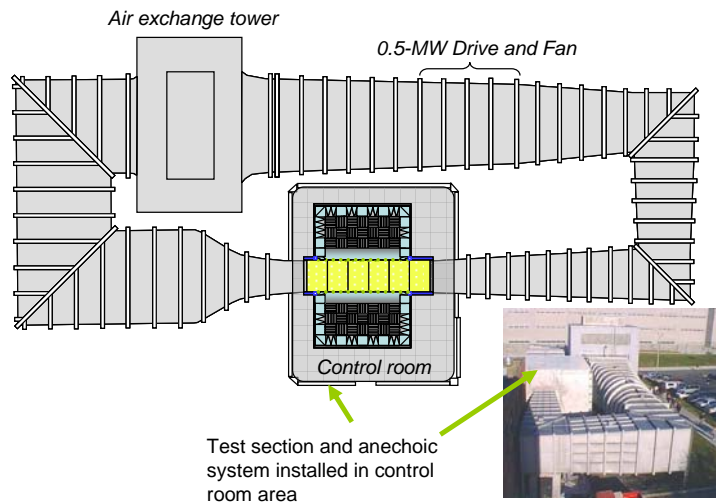


Figure 1. Plan view of the VT Stability Wind Tunnel layout.

contraction nozzle, which further reduces turbulence levels and accelerates the flow to test speed. At the downstream end of the test section, flow passes into a 3-degree diffuser. Sixteen 0.16-m high vortex generators arranged at intervals of 0.39 m around the floor, walls, and ceiling of the flow path, at the entrance to the diffuser, serve to mix momentum into the diffuser boundary layer, minimizing the possibility of separation and the consequent instability and inefficiency. The four corners in the flow path (two between the air exchange tower and settling chamber, and two between diffuser and fan) are equipped with diagonal arrays of shaped turning vanes. Spacing between the vanes is 0.3 m except in the corner immediately ahead of the settling chamber where the spacing is 0.076 m.

The test section itself is located in a hermetically sealed steel building. The pressure inside this control room is equalized with the static pressure in the test section flow, this being below atmospheric by an amount roughly equal to the dynamic pressure. Pressure is equalized through a small aperture in the tunnel side wall at the upstream entrance to the diffuser.
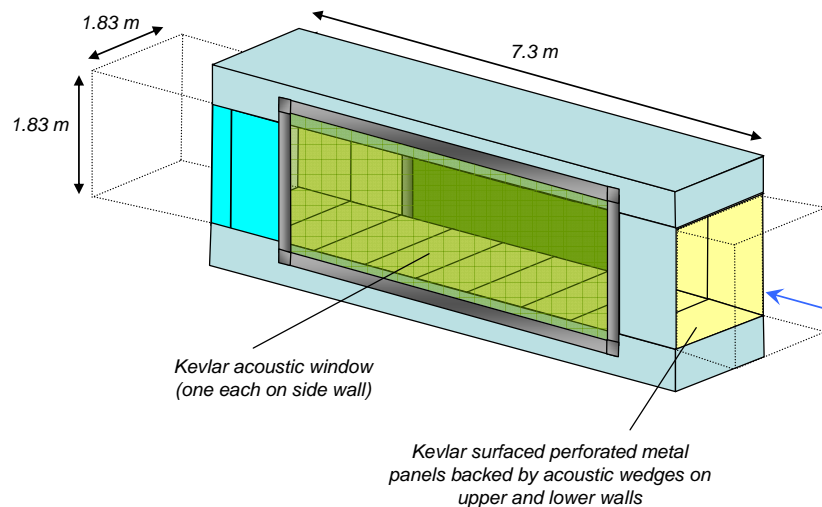
Flow through the empty test section (measured with a hard-walled test section in place) is both closely uniform and of very low turbulence intensity. Turbulence levels are as low as 0.016% at 12 m/s and increase gradually with flow speed to 0.031% at 57m/s.

**B. Anechoic System**

The anechoic system consists, primarily, of an acoustic test section and two large anechoic chambers. The system is unique in two respects. First, tensioned Kevlar cloth is used to separate flow in the test section from the anechoic chambers, eliminating the need for a jet catcher and reducing aerodynamic interference. Second, the entire system is removable so that the wind tunnel can be switched from an anechoic to a hard-walled configuration and back again.

The 7.3-m-long acoustic test section is depicted in Figure 2. This test section defines the same flow path as the hard-walled test section but is expressly designed for aeroacoustic testing. The upper and lower walls of the test section consist of a series of perforated steel sheet panels bonded to a layer of Kevlar cloth that forms a smooth, quiet, but acoustically transparent flow surface. The volume of the cavities behind the



1.83 m

1.83 m

7.3 m

Kevlar acoustic window (one each on side wall)

Kevlar surfaced perforated metal panels backed by acoustic wedges on upper and lower walls

**Figure 2. Schematic of the new acoustic test section.**

floor and ceiling panels was filled with 0.457-m-high foam wedges, which would be expected to eliminate acoustic reflections at frequencies above 190 Hz. The sidewalls of the test section are dominated by two large Kevlar cloth acoustic windows. The windows consist of tensioned thin weave Kevlar 120® cloth (7.9 grams/cm$^2$), covering a total streamwise length of some 6 m and the full 1.8-m height of the test section. The Kevlar cloth forming the acoustic windows is mounted and stretched on 5.37×2.51-m tensioning frames to a tension of the order of 0.5 tonnes per linear meter. Sound passes through the Kevlar acoustic windows with almost no attenuation over a large frequency range.
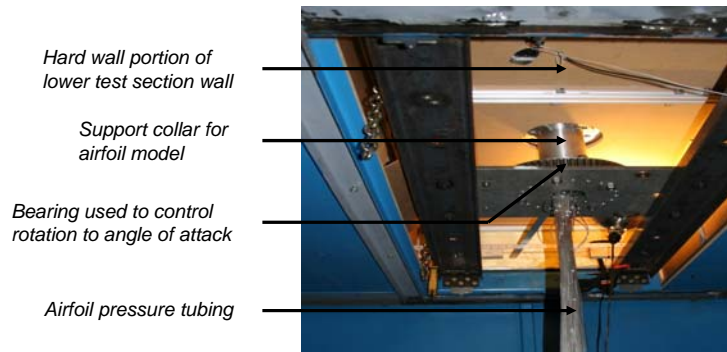
The upper and lower walls contain hardware for the vertical mounting of two dimensional airfoil models (e.g. Figure 3) midway between the acoustic windows (i.e. test section side walls) and 3.56 m from the upstream end of the test section.
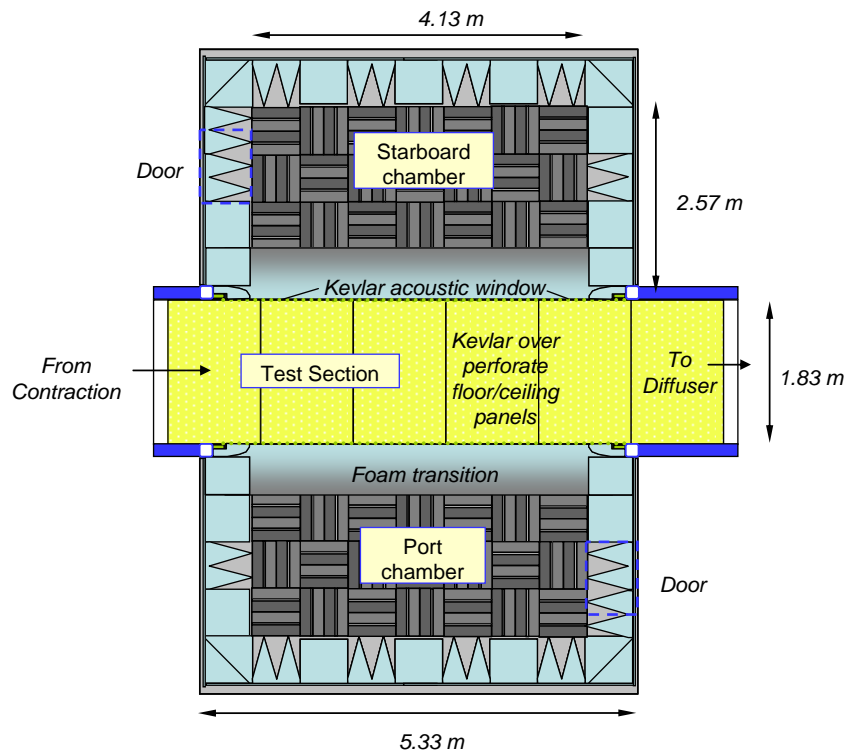
Anechoic chambers are mounted on either side of the anechoic test section to capture the sound emitted through the acoustic windows, as depicted in Figure 4. Each chamber has a streamwise length of 6 m, extends 2.8 m out from the acoustic window, and has a depth of 4.2 m. The chambers are lined with 0.610-m high acoustic wedges expected to eliminate acoustic reflections above 140 Hz.



**Figure 3. Photograph taken from beneath the test section showing the collar and bearing arrangement that form the airfoil mount and mechanism for changing the angle of attack.**

The anechoic system was first completed and installed in the facility in August 2006, and initial observations were made concerning its performance with a view to opportunities for improvement. In-flow noise levels in the new test section were found to be 5 to 10 dB below those in the original hard-walled test section. While this was satisfying, it was felt that significantly greater reductions should be possible with the treatment of the wind tunnel fan and the rest of the flow circuit. Furthermore, problems with seaming of the Kevlar meant that it could only be a fraction (about 10%) of the intended tension.



**Figure 4. Horizontal cross section through the assembled anechoic system showing the acoustic test section and anechoic chambers.**

## C. Acoustic Treatment of the Wind Tunnel Circuit and Test Section Improvements

Previous work[3] had identified the fan as a major noise source in the tunnel circuit. Acoustic treatment was therefore directed at the fan and at the walls of the tunnel duct between the fan and the test section. The areas treated are shown schematically in Figure 5. At periodic intervals throughout the treatment, the in-

flow noise in the hard-walled test section configuration was re-measured and compared with original levels. 1-Hz-bandwidth noise spectra measured at the test section center are plotted in Figure 6.
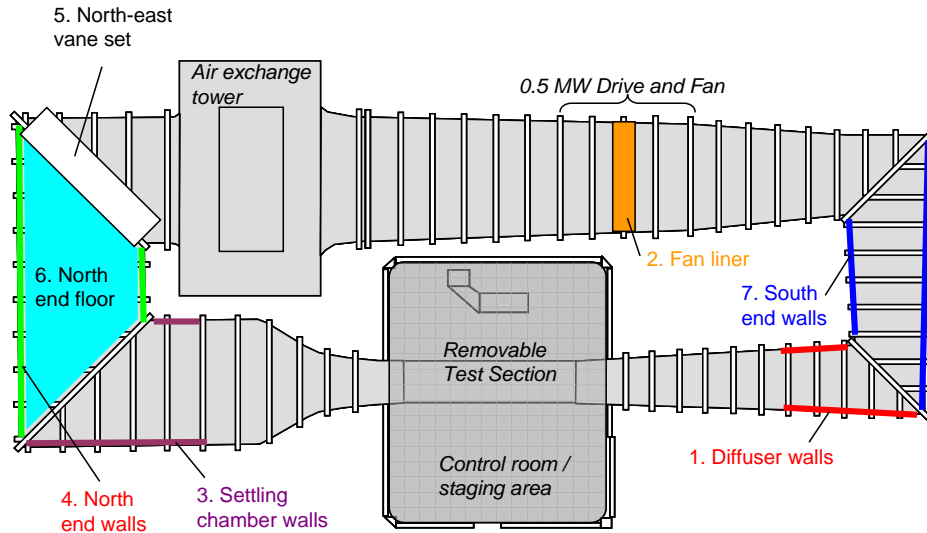


**Figure 5. Schematic showing the location of acoustic treatment applied to the tunnel circuit.**
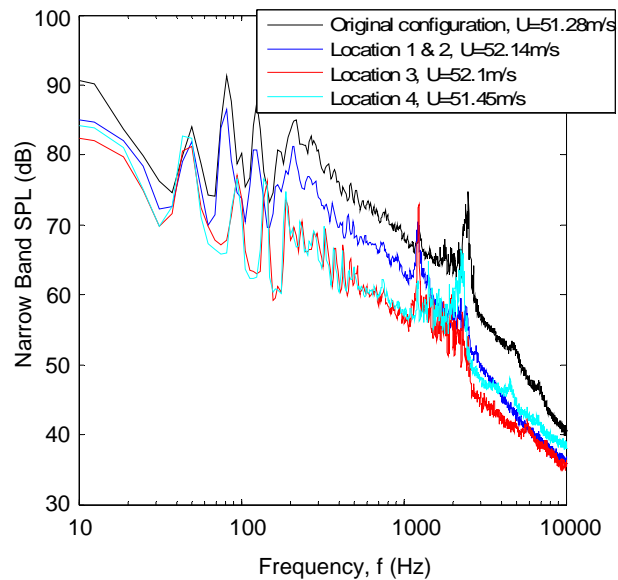
The following treatment was applied:

Location 1: Melamine foam lining (5-cm thick) applied to the downstream ends of the sidewalls of the diffuser. About 28 m$^2$ of self-adhesive foam was used with the idea of absorbing high frequency noise coming upstream from the fan.

Location 2: Variable thickness foam liner installed around the fan blade tips to reduce tip noise. Phased-array measurements of the fan had shown that the fan tip gaps were a major source of noise. The foam liner was custom manufactured to reduce the tip gap by about half. In addition, a wire mesh model catcher just upstream of the fan was removed. As shown in Figure 6, the diffuser and fan treatments alone produced about a 5 to 6 dB reduction across the entire frequency range.

Location 3: A 5-cm thick urethane foam liner was installed on the walls of the settling chamber, covering about 56 m$^2$. This liner produced substantial further reductions of up to about 6 dB, particularly below 1 kHz.



**Figure 6. Inflow noise levels measured before and after acoustic treatment in the tunnel circuit.**

Location 4: A 5-cm thick urethane foam liner was installed on the walls of the northern leg of the flow circuit, upstream of the settling chamber, covering about 74 m$^2$ of wall space. Measurements (Figure 6) show a further 1-dB reduction at frequencies below 1 kHz, but a significant increase at higher frequencies. It seems unlikely that this increase was directly produced by the additional treatment or its effects on tunnel circuit losses, since flow speeds in the northern leg of the circuit would have been very low. As discussed below, it seems probable that at the reduced noise levels achieved with the acoustic treatment, noise

generated by the in-flow microphone stand was significant and quite a strong function of the exact placement of the stand. These are suspected to be the sources of the increased noise levels at high frequency.

Location 5: Extensive work was undertaken to acoustically treat the 3 by 7.6-m north-east vane set that follows the fan. The geometry of the turning vanes was measured and a panel method was used to determine the pressure distribution around the vanes profile. The effects of thickening the vane section in various ways were then investigated using the panel method. The final configuration, which includes 2.5-cm thick shaped melamine foam applied to the pressure side of the vane, was chosen because it appeared to have no adverse effects on the pressure distribution while providing an acoustically absorbent flow surface that faced the fan.

Locations 6 and 7: Following the vane treatment, 5-cm urethane foam was also applied to the floor of the north leg of the tunnel circuit (adding about 37 $m^2$ of treatment), and to the walls of the southern leg of the circuit, continuous with the diffuser treatment (about 28 $m^2$). Note that, because of timing issues, the acoustic effects of the treatment at locations 5, 6 and 7 could not be assessed separately but, instead, were assessed along with other modifications during the second installation of the anechoic system discussed below.
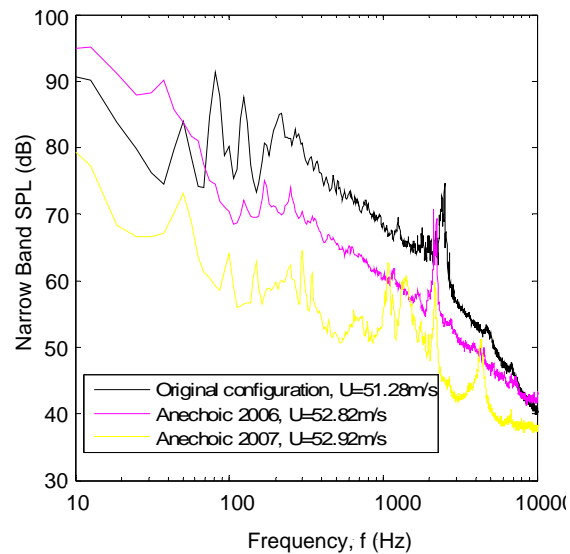
In addition to the above, significant work was also done to optimize the characteristics of the test section. Additional acoustic absorbers were incorporated into the test section side walls upstream and downstream of the Kevlar acoustic windows. Melamine foam backing was installed above and below the upper and lower flow surfaces to prevent the airflow through the acoustic treatment. Furthermore, C&C Sailmakers of Texas were contracted to sew new Kevlar acoustic windows using iteratively designed seams that could take much higher load. This enabled the windows to be placed under full tension in subsequent tests.

## III. Final Anechoic Facility Characteristics

### A. Background Noise Levels

Figure 7 compares in-flow acoustic measurements made after the re-installation of the anechoic system (with all the improvements described in Section II.C), with acoustic levels measured during the initial installation and in the original hard-walled configuration at about 50 m/s, for example, (similar results have been obtained at other speeds). Measurements were made at the center of the test section. Levels are down across the spectrum by as much as 12 dB compared to the initial anechoic installation, and as much as 25 dB compared to the original hard-walled configuration. Note that these results underestimate the true noise reduction because of the influence of noise generated by the microphone stand. This can be seen in measurements of noise levels in the anechoic chambers as a function of flow speed shown, for example, in Figure 8. Measurements made with the microphone stand in the test section show levels that are between 3 and 25 dB higher between 300 Hz and 10 kHz than when the stand is removed. Indeed, it seems probable that above 300 Hz the inflow noise spectra shown in Figure 7 for the newly treated anechoic test section are dominated by noise from the microphone stand.



**Figure 7. Comparison of inflow acoustic levels in the original hard-walled test section, during the initial anechoic system installation, and in anechoic configuration after treatment of the test section and flow circuit.**
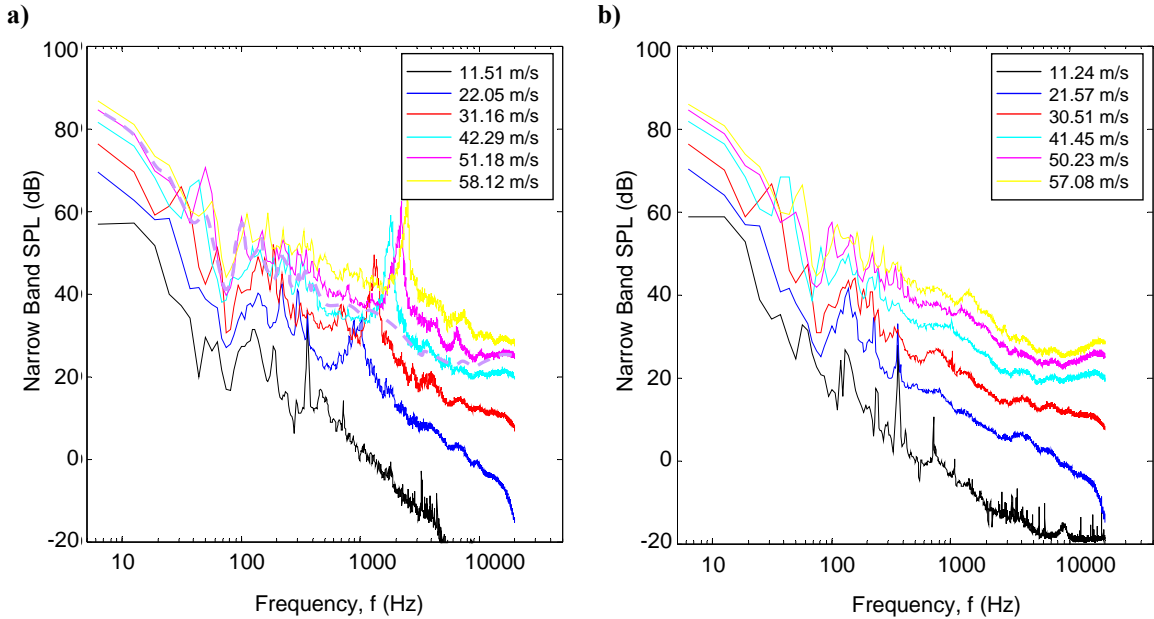
Confirmation of just how much quieter the newly treated facility is can be seen in Figure 9. Here, out of flow noise levels (with no microphone strut present) are compared with those measured during the initial

anechoic system installation. Levels are greater than 10 dB down between 300 Hz and 10 kHz and 15 dB down between 500 Hz and 5 kHz.

a)

b)



**Figure 8. Noise levels measured in the starboard-side anechoic chamber as a function of flow speed, a) with the inflow microphone stand in the test section and b) empty test section. Dashed line in a) shows empty test section levels at 50.23 m/s, for direct comparison.**
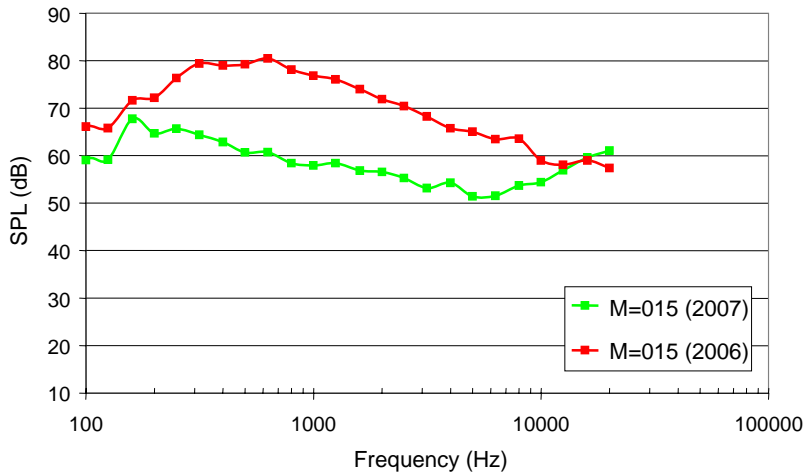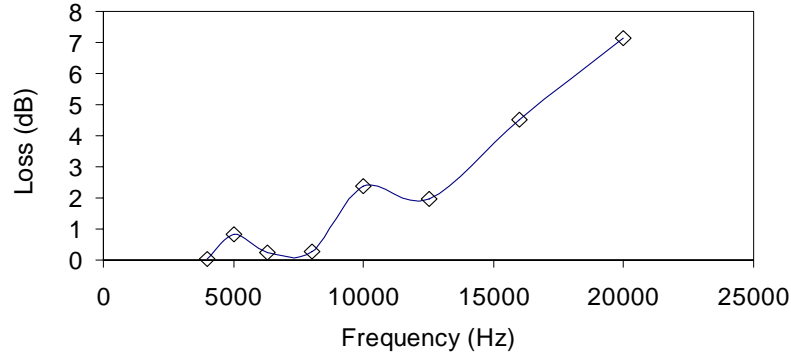


**Figure 9. Noise levels measured on the port-side anechoic chamber using a single microphone comparing levels from the initial installation (2006) with those from the current installation (2007) after acoustic treatment.**

## B. Acoustic Transparency of the Kevlar Windows.

A detailed description of the procedure followed to determine the sound loss through the Kevlar windows may be found in reference [6]. The procedure is briefly summarized in the following.

A sound source with an operating range of 1.5-18 kHz and driven with white noise was used to determine the sound loss through the Kevlar window. The radiation of the source was characterized in an anechoic chamber. A single microphone was used to record the sound pressure of the source over a semi-spherical surface with radius 52 cm. The source was small enough for the microphone to be in the geometric and acoustic far-field for the range of frequencies considered. After this calibration, the source

was mounted at the center of the test section. A single calibrated microphone was installed in the starboard-side chamber, straight in front of the source, about 2 m from the Kevlar window, to record the levels generated by the source. The levels this microphone would have read in the absence of the Kevlar window were predicted. The noise



**Figure 10. Loss in dB through the Kevlar windows as a function of frequency.**

spectrum of the source obtained from the calibration procedure in an anechoic chamber was extrapolated to the distance between the source and the microphone in the wind tunnel, by the means of the spherical spreading law. The predictions were compared to the measurements to determine the loss through the Kevlar window. Results are reported in Figure 10 in one-third octave band. The loss through the Kevlar is relatively low from low frequencies to about 8 kHz, e.g. less than 1 dB. In the frequency range 8-20 kHz, the loss increases from 1 to 7 dB. Noise measurements of actual models installed in the test section may be corrected for the loss through the Kevlar window using curves such as the one presented in Figure 10.

### C. Aerodynamic Performance of the Empty Anechoic Test Section

Measurements were performed on the empty acoustic test section to characterize the aerodynamic performance of this configuration. These measurements include: upstream and downstream boundary layer profiles with associated displacement and momentum thicknesses, Kevlar acoustic window deflection at several flow speeds, and pressure distributions over the acoustic windows. The majority of the data collected regarding the window performance was taken at two nominal speeds: 30 m/s and 50 m/s.
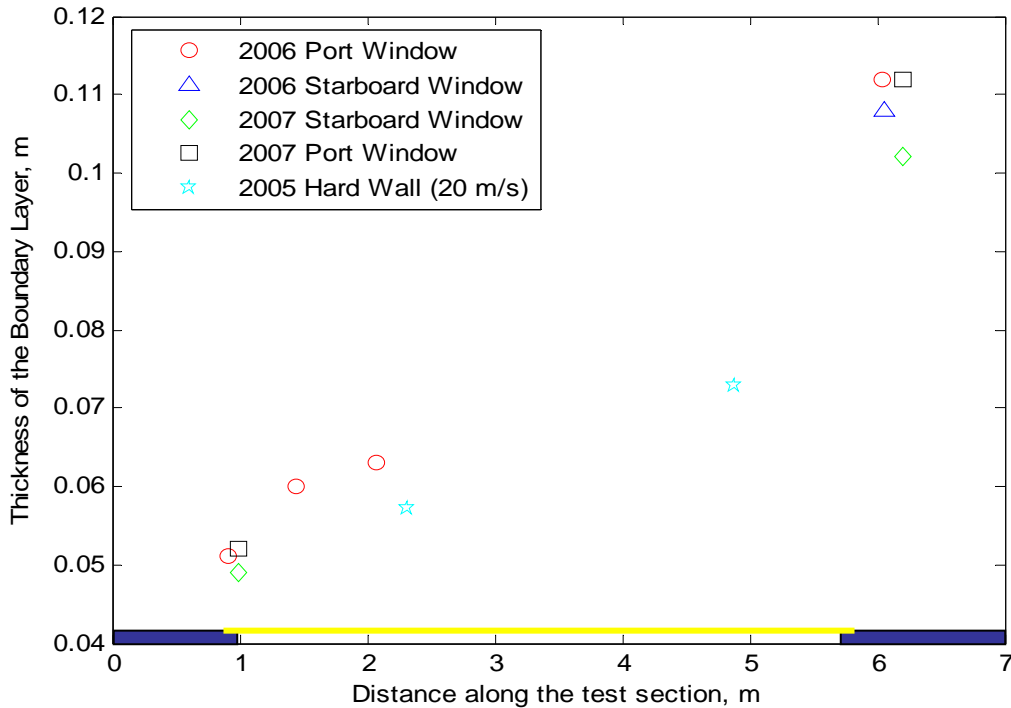
The boundary layer measurements were completed using a probe rake designed with five straight pitot static probes of 0.432-m length and 3.175-mm diameter. These were mounted horizontally (or vertically depending on measurement location) to a sting attached to a traverse controlled by three PDX-13 controllers. The sting was mounted on the traverse to extend the probe tips a full 2 m ahead of the traverse. Measurements were taken at the entrance and exit of the test section (0.762 m and 6.55 m from its upstream end) to compare the boundary layer thickness to that of the hard-walled configuration.

Boundary layer thickness values were determined at the center of the four exit walls of the test section at 30 m/s and 50 m/s and at the center the four entrance walls at 30 m/s. Table 1 contains the boundary-layer thickness values $\delta$, as well as the displacement thicknesses $\delta^*$, for the conditions measured for the final facility configuration. In Figure 11, the boundary layer thicknesses measured on the port- and starboard-side walls are compared with similar measurements made in 2005 in the hard-walled test section, and in 2006 during the initial anechoic test section installation, for which the Kevlar windows could not be fully tensioned. The hard-wall data was taken at a nominal flow speed of 20 m/s, which is considerably lower than for the other cases, and is shown only as a reference. Boundary layer thickness values at the inlet, upstream of the acoustic windows, vary by 3 mm or less between the different configurations, and are consistent with the hard-wall values referenced in Figure 11. The blue sections in the lower portion of the plot indicate the edge of the steel panels at the upstream and downstream ends of the test section. The yellow line connecting the two represents the test section length covered by the Kevlar windows. Boundary layer thicknesses at the exit of the test section are the same for the initial and final acoustic test section configurations, but the rate of growth is faster than that seen with the hard wall, presumably because of the porosity of the Kevlar windows. The boundary layer thickness is about 30% greater at the back of the test section in anechoic configuration. This additional boundary layer growth would be expected to produce an additional acceleration of the free stream of between 0.5 and 1% over the length of the test section.

**Table 1. Boundary Layer thickness values for the empty test section at nominal flow speeds of 30 and 50 m/s on the four walls of the inlet and exit.**

| Location | Velocity (m/s) | δ (mm) | δ* (mm) |
|---|---|---|---|
| Inlet Floor | 27.3 | 54.1 | 6.7 |
| Inlet Ceiling | 29.4 | 49.0 | 6.8 |
| Inlet Starboard Wall | 28.1 | 49.0 | 5.3 |
| Inlet Port Wall | 28.7 | 52.0 | 5.3 |
| Downstream Floor | 30.5 | 110.0 | 12.4 |
| Downstream Floor | 49.5 | 118.0 | 19.2 |
| Downstream Ceiling | 30.0 | 107.0 | 13.1 |
| Downstream Ceiling | 48.7 | 122.9 | 16.9 |
| Downstream Starboard Wall | 29.6 | 102.1 | 12.6 |
| Downstream Starboard Wall | 49.4 | 106.2 | 15.5 |
| Downstream Port Wall | 29.8 | 112.0 | 12.3 |
| Downstream Port Wall | 49.3 | 123.0 | 16.5 |



**Figure 11. Growth of the boundary layer along the test-section walls for a nominal flow speed of 30 m/s at various configurations.**

   Measurements were made of the mean deflection of the Kevlar acoustic windows in final configuration. Twenty-eight discrete measurements arranged in a grid pattern were taken along the inside of both test section windows with the tunnel running at 30 m/s and 50 m/s. Figure 12 shows the deflection of the Kevlar windows measured for a nominal flow speed of 30 m/s, for a) the starboard-side and b) the port-side windows. The start and end of the Kevlar windows are marked by vertical lines (91 cm and 585 cm

approximately). Note that the maximum mean deflection of the windows is of the order of 1 cm. No significant window vibration was observed.
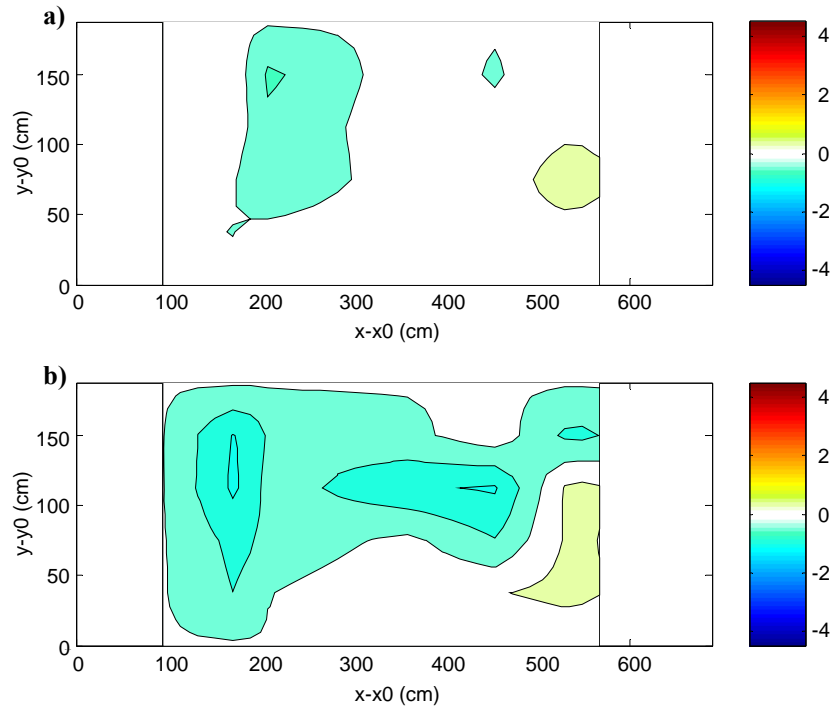


**Figure 12. Deflection of the Kevlar windows (in cm) measured for a nominal flow speed of 30 m/s, for a) the starboard-side and b) the port-side windows.**

Similar measurements of the mean pressure difference across the acoustic windows (between the interior of the test section and the anechoic chambers) were made using a traversable array of Pitot static probes. Five straight Pitot static probes (3.175 mm diameter), measuring 0.432 m in length, were attached to an aluminum extrusion spanning the length of the port side of the test section. These probes were attached to the rail via aluminum stand-offs (0.305-m high) that could slide to various positions along the rail and be locked in place. Static pressure coefficients (CPS) were measured at eight streamwise positions along the window, and at three window heights (0.343 m, 0.953 m, and 1.359 m above test section floor) for nominal tunnel speeds of 30 and 50m/s. Static pressure coefficients for each anechoic chamber were determined simultaneously, and the static pressure difference across the window was plotted as a function of the streamwise position along the length of the test section. Analysis of this pressure data showed static pressure values that were quite large, indicating flow patterns that were not predicted by the measured boundary layer growth. To determine what was causing this pressure field, a calibration of this system was preformed in the hard-walled test section to ascertain the baseline flow properties and determine the contribution of the probes and the boundary layer growth to the measured pressure field from the anechoic test section. The rail system was assembled in the hard-walled test section at the same location as for the tests in the anechoic test section, and the entire test matrix was repeated for the port-side window pressure measurements. The original anechoic data could then be corrected using the calibration data acquired in the hard-wall test.

Sample measurements, in Figure 13, show static pressure coefficient variations over the window to be small for the empty test section. There is some pressure variation along the length of the window that is most likely a result of the boundary layer growth, and/or interaction of the flow with the leading and trailing edge regions of the window.
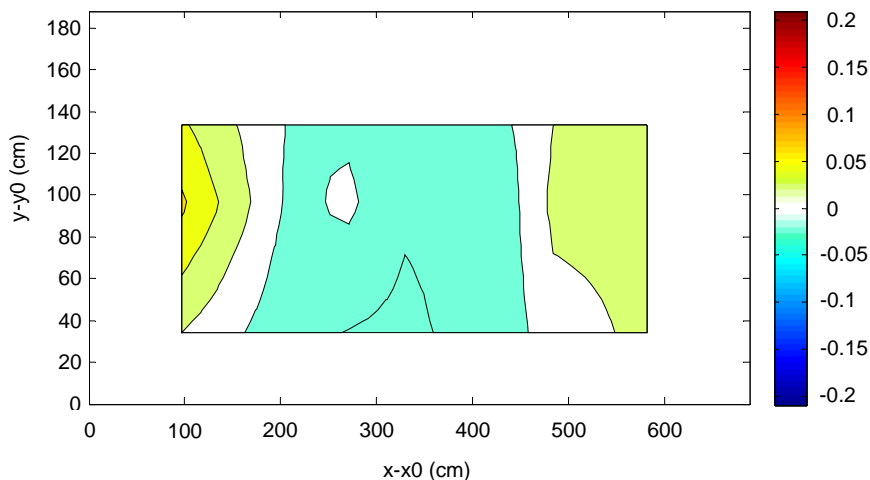
**Figure 13. Contour plot showing the net static pressure coefficient difference across the port-side window at a nominal speed of 30 m/s in the empty test section.**

Similar window pressure and window deflection measurements were preformed on the NACA 0012 model and are discussed in the next section.
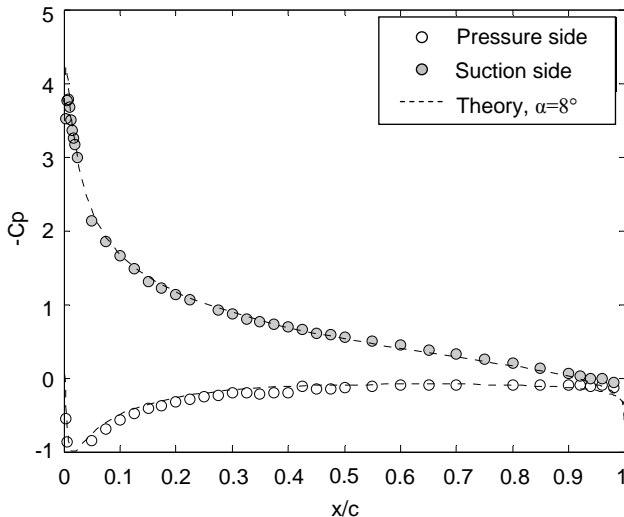
## IV.   Wind Tunnel Tests on NACA 0012 Airfoils

### A.  Aerodynamic Measurements

Further aerodynamic calibration of the facility was performed using a 0.91-m-chord, 1.83-m-span, NACA 0012 airfoil model. The model was mounted vertically with its quarter chord in the streamwise center of the test section, midway between the port-side and starboard-side acoustic windows 3.54-m downstream of the forward end of the test section and 2.63 m downstream of the acoustic window leading edges. This model features 81 pressure ports arranged along the model mid span.

Aerodynamic measurements with the model include mean pressure distribution as a function of angle of attack (used to infer the lift interference correction), test-section boundary layers, and deflection of and pressure distribution over the two acoustic windows. Figure 14 shows a sample pressure distribution measured at a geometric angle of attack of some 10.4



**Figure 14. Pressure distribution for the NACA 0012 model at 8 degrees effective angle of attack, Re = $1.53 \times 10^6$.**

degrees. Comparison with the panel method solution also shown in the figure suggests an effective angle of attack of 8 degrees, confirming a -22% interference correction. This is significantly less than the correction that would be expected for a model of this size in a free jet, of -50% (computed from the method of Brooks et al.[5]) or -73% (computed using the method of Barlow et al.[7]), confirming the usefulness of the acoustic windows in this regard.

**Table 2. Boundary Layer thickness values for the NACA 0012 Model on the test-section walls,**
**6.55 m downstream of the test section entrance**

| Location | Flow Speed (m/s) | δ (mm) | δ* (mm) |
|---|---|---|---|
| NACA 0012 at 0 AOA Port Wall | 29.0 | 134 | 30.2 |
| NACA 0012 at 8 AOA Port Wall | 28.1 | 211 | 21.3 |
| NACA 0012 at 0 AOA Starboard Wall | 29.3 | 130 | 23.6 |
| NACA 0012 at 8 AOA Starboard Wall | 28.1 | 212 | 58.6 |

The boundary layer thickness and the deflection of the Kevlar windows with the NACA 0012 installed were determined in the same manner as for the empty test section. Measurements were taken at the entrance and exit of the test section (0.762 m and 6.55 m from its upstream end) to compare the boundary layer thickness to that of the empty test section. The results of these boundary layer measurements are given in Table 2. Figures 15 and 16 show the deflections of the Kevlar acoustic windows forming the tunnel sidewalls in the presence of the NACA 0012 airfoil, at a flow speed of 30 m/s, with the model mounted at a 0- and 8-deg effective angle of attack. At zero angle of attack, the walls are displaced outward from the test section ahead of the airfoil, and drawn inward downstream. With the angle of attack at 8 degrees, the window is drawn into the test section on the suction side of the test section and displaced outward on the pressure side, much as one might expect. The maximum deflection remains no more than about 4 cm. No significant window vibration was observed.
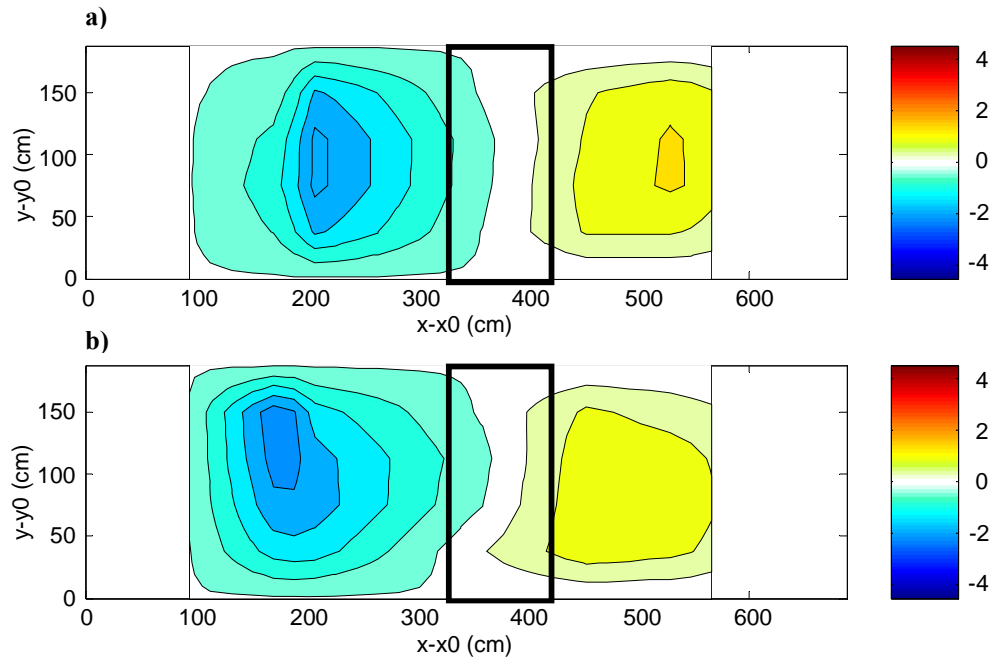


**Figure 15. Window deflection (in cm) at nominal 30-m/s flow speed, with the NACA 0012 airfoil at 0-deg effective angle of attack, for a) the starboard-side and b) the port-side windows.**
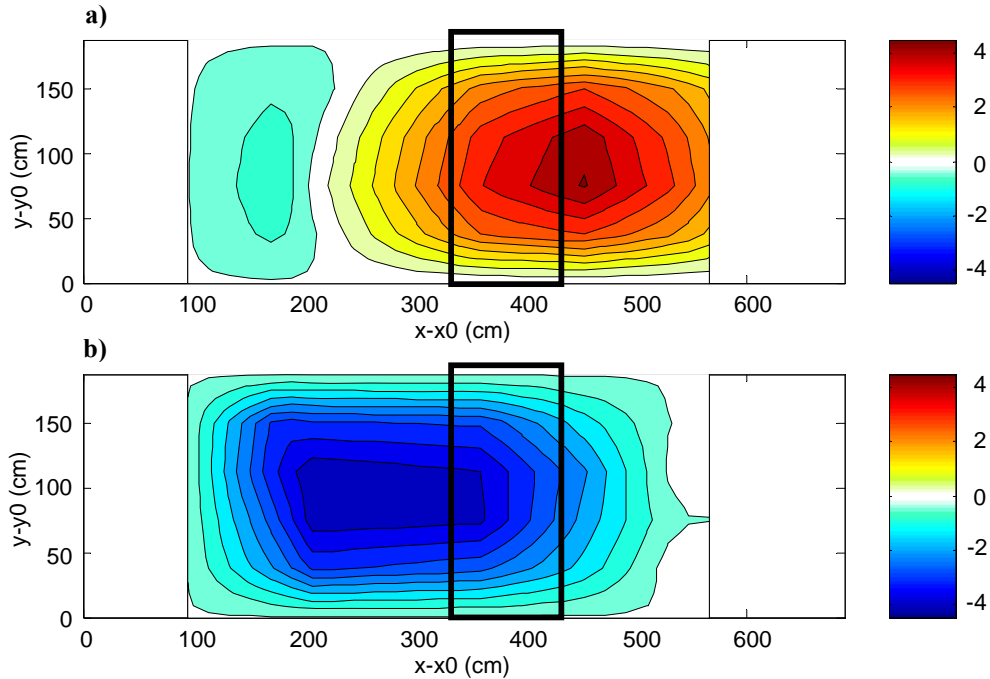
**Figure 16. Window deflection (in cm) at nominal 30-m/s flow speed, with the NACA model at 8-deg effective angle of attack, for a) the starboard-side and b) the port-side windows.**

Measurements of the pressure differences (which here have been offset to account for empty-test-section flow acceleration associated with the boundary layer growth) across the acoustic windows were compared to a panel method calculation of the test section airfoil flow, modified to account for the porosity of the acoustic windows. Figures 17a and b show the static pressure difference across the port-side window for a nominal flow speed of 30 m/s, with the airfoil at a) 0-deg and b) 8-deg effective angle of attack. Measurements were carried out at three heights, 0.343 m (green circles), 0.953 m (blue circles), and 1.359 m (red circles) above the test section floor. Note that for these plots the zero location is the quarter chord of the model, with negative $x$ (m) values upstream of the model.
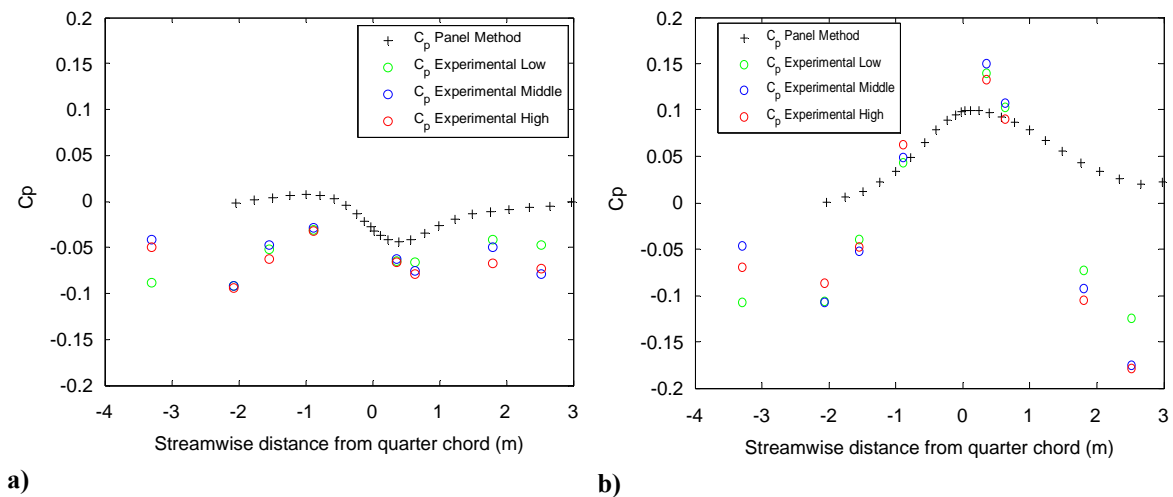


**Figure 17. Static pressure difference across the port-side window for a nominal flow speed of 30 m/s, with the airfoil at a) 0- and b) 8-deg effective angle of attack.**

The general trend in the static pressure coefficient is correctly predicted by the panel method for both of these cases. However there are some slight variations in the magnitude of the pressure gradient in the experimental data compared to the panel method results. The regions of the windows that are directly adjacent to the model show good agreement, suggesting that the general inputs in the panel method (porosity approximation) and boundary conditions are adequate. The areas upstream of the model, near the inlet, have pressures that are lower than those predicted by the panel method. This is suspected to be a result of the window deforming upstream of the model, a phenomenon that the panel method does not currently account for. The region of the window that is downstream of the model has flow speeds that are faster (lower pressures) than those predicted by the panel method as well. Wall deflection may also be a factor here, but additional boundary layer growth associated with the pressure gradients imposed by the airfoil may also be to blame. The displacement thickness values measured with the airfoil suggest an additional acceleration of about 3% produced by this blockage which would result in a fall in the static pressure coefficient of about -0.06.

The addition of the window deflection to the porous walls of the panel method, as well as the investigation of modeling the boundary layer effects will be the subject of future work.

## B. Aerocoustic Measurements

Aeroacoustic measurements were conducted on a 20-cm-chord, 1.83-m-span, NACA 0012 airfoil. Tests were performed for a range of angles of attack, flow speeds, and trip conditions.
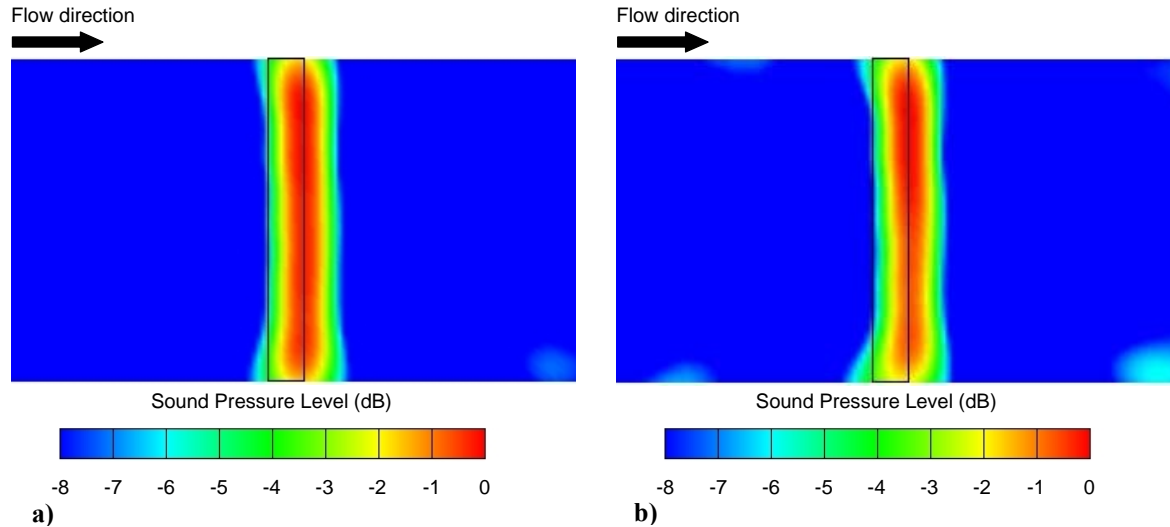
The 63-element microphone phased-array depicted in Figure 18 was used for noise source location and to determine the levels of self-noise from the airfoil exposed to the flow. This array has a star configuration consisting of 7 arms with 9 microphones per arm. The array has an inside diameter of 25 cm and an outside diameter of 1.52 m. The array center body is provided with a laser pointer that projects a laser dot along a line perpendicular to the array plane passing through the array origin. This laser pointer was used for alignment purposes. Measurements were made using the array located on the port-side chamber, 2.64 m from the test section center (1.72 m from the port-side acoustic window). The array center was pointing toward the airfoil rotation axis, at the midspan. The 63 microphone signals were sampled simultaneously at 51,200 samples per



**Figure 18: Photograph of the 63-element microphone phased-array.**

second in 25 separate blocks of 16,384 samples each. Time-domain data were processed in one-third octave bands using a frequency-domain, phased-array, beamforming code developed at Virginia Tech that accounts for the flow in the test section and the sound refraction through the flow velocity discontinuity between the test section and the anechoic chamber. Diagonal removal was used in the post-processing of the phased-array data to minimize the effects of the background noise. Phased-array data were processed in one-third octave bands from 500 to 5040 Hz.

Figure 19a and b show sample beamforming maps obtained at 2500 Hz, for the 20-cm-chord airfoil at effective angles of attack of 0 and 5.3 degrees. The flow speed in the test section was 40.5 m/s (M = 0.117), which corresponds to a chord Reynolds number of $5x10^5$. The boundary layer was tripped from the leading edge to 20%-chord. The maps show an extremely clear noise source at the trailing edge of the airfoil at the two frequencies shown.

Flow direction

Sound Pressure Level (dB)

-8  -7  -6  -5  -4  -3  -2  -1  0

a)

Flow direction

Sound Pressure Level (dB)

-8  -7  -6  -5  -4  -3  -2  -1  0

b)

**Figure 19. Beamforming maps in one-third octave bands at 2500 Hz of the trailing edge noise produced by a 0.2-m-chord tripped NACA 0012 airfoil at a chord Reynold number of 5x10⁵, at a) 0- and b) 5.3-deg effective angle of attack.**

Aeroacoustic testing of NACA 0012 airfoils have been conducted in the past by Brooks *et al.*[5] in the low-turbulence potential core of a free jet located in an anechoic chamber. The jet was provided by a vertically mounted nozzle with a rectangular exit with dimensions of 30.48×45.72 cm. Acoustic measurements were carried out for a range of airfoil geometries, angles of attack, tripp conditions, and flow speeds. Six microphones were mounted in a plane perpendicular to the airfoil midspan, at radii of 1.22 m from the trailing edge. Two of them were perpendicular to the chord line at the trailing edge for an effective angle of attack of 0 degree. The other microphones were positioned 30 degrees forward and 30 degrees aft. Cross-spectra between the microphones were used to determine the self-noise emitted from the trailing edge. Corrections were applied to the spectra to account for sound refraction through the shear layer and for trailing-edge noise directivity effects. The noise measured was that for an observer positioned perpendicular to, and 1.22 m from, the trailing edge and the model midspan. Acoustic results obtained from tests conducted on a 45.72-cm-span, 22.86-cm-chord airfoil are considered here since they can be directly compared to the results obtained in the herein study.

Self-noise spectra for the 20-cm-chord airfoil tested in the VT Stability Wind Tunnel were determined by integration of the beamforming maps. Integrated spectra are obtained by adding the levels on the beamforming maps and normalizing such levels by the point spread function of the phased array over the desired region. Also, a threshold of 3 dB from the peak value is used to reduce the influence of extraneous noise sources. The volume of integration was a rectangular cube emcompassing the trailing edge with dimensions of 45.72-cm in the spanwise direction and 30.48x30.48-cm in the streamwise and lateral directions. The volume was symmetric to the midspan and to the chord line for the airfoil at 0-deg angle of attack. Corrections were applied to the spectra to account for the sound loss through the Kevlar windows. Data were also corrected using the spherical-spreading law to match the position of the observer in Brooks *et al.*[5]'s experiments.

Figures 20a and b compare trailing edge noise spectra in one-third octave band measured by Brooks *et al.*[5] (solid black lines) for a 22.86-cm-chord airfoil and measured in the VT Stability Wind Tunnel for a 20-cm-chord airfoil (red solid dots), at angles of attack of a) 0 and b) 5.3 degrees. The flow speeds in the open-jet and VT wind tunnels were 39.6 m/s and 40.5 m/s, respectively. The boundary layers of the airfoils were tripped from the leading edge to 20%-chord. Spectra obtained in the VT wind tunnel were truncated below 1000 Hz, and above 4000 Hz. For frequencies below 1000 Hz, beamforming maps are dominated by strong noise sources at the junction of the airfoil with the test-section floor and ceiling. For frequencies above 4000 Hz, results are not reliable because of the large size of the array and the fact that the array was not calibrated for phase. Results obtained in the VT wind tunnel are in very good agreement with those obtained by Brooks et al.[5] A maximum difference in levels of about 6 dB is observed, which is remarkable given that the tests were conducted in different wind tunnel facilities, using different methods to compute

the self-noise levels. Spectra levels for the untripped cases (not depicted here) obtained in the open-jet and VT wind tunnel exhibit similar pattern, but differ significantly in terms of levels. The reason for these discrepancies has not been established yet.

a)



b)
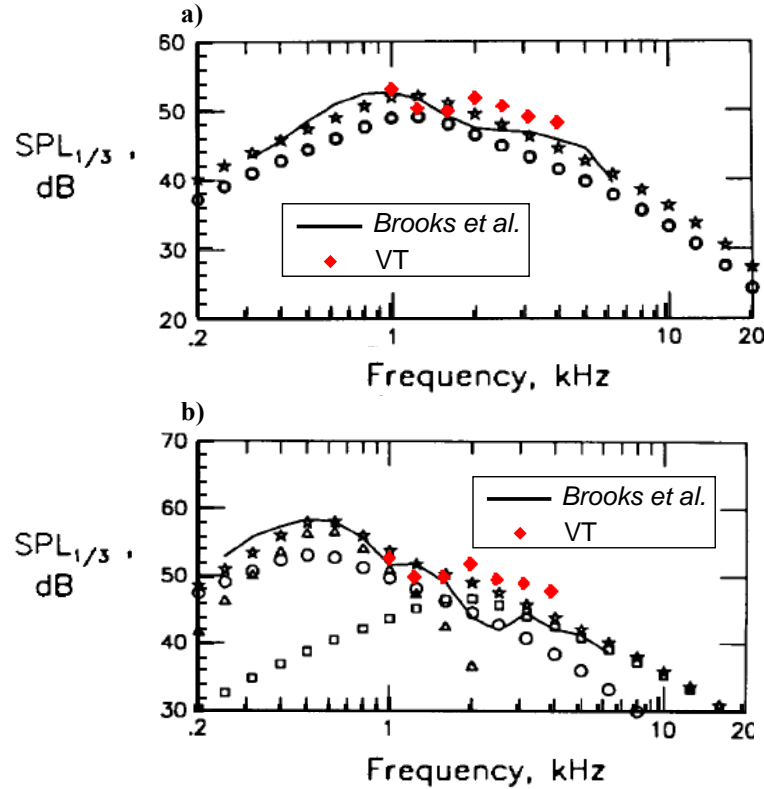


**Figure 20: Trailing edge noise spectra in one-third octave band measured by Brooks et al.[4] (solid black lines) in an open-jet wind tunnel for a 22.86-cm-chord airfoil in flow with a speed of 39.6 m/s and measured in the VT Stability Wind Tunnel for a 20-cm-chord airfoil (red solid dots) in a flow with a speed of 40.5 m/s, at angles of attack of a) 0 and b) 5.3 degrees.**

## V.  Conclusion

The new Virginia Tech anechoic wind tunnel was described. This facility includes a novel Kevlar-walled test section. The Kevlar walls are transparent to sound, eliminate the need for a jet catcher, and significantly reduce aerodynamic interference. The facility is also unique in that the anechoic system can be removed and the aerodynamic test section and capability restored.

Extensive work has been conducted to reduce background noise levels in the facility, including treatment of the wind tunnel fan, the flow circuit, and the test section. This has resulted in a reduction of background noise levels of as much as 25 dB compared to the original hard-walled configuration of the facility. Aerodynamic measurements with a series of airfoil models in the test section showed interference corrections to be less than half those expected in a free jet. Some of this interference is visible in small deflections of the Kevlar windows and the pressure differences exerted across them. These appear consistent with panel method calculations for the test section and model. Phased array measurements of trailing edge noise have been made in the facility for a range of conditions. Analysis of these data shows high signal-to-noise ratios. Spectra levels of the trailing edge noise were computed and compared to those obtained in past experiments in an open-jet wind tunnel. Results are in very good agreement for the case of tripped boundary layer.

## Acknowledgments

## References

[1]Jaeger, S. M., Horne, W. C., and Allen, C. S., "Effect of Surface Treatment on Array Microphone Self-Noise," *6th AIAA/CEAS Aeroacoustics Conference*, Lahaina, HI, June 12-14, 2000. AIAA-2000-1937

[2]Ravetta, P. A., Burdisso, R. A., and Ng, W. F., "Wind Tunnel Aeroacoustic Measurements of a 26%-scale 777 Main Landing Gear," *10th AIAA/CEAS Aeroacoustics Conference*, Manchester, Great Britain, May 10-12, 2004. AIAA-2004-2885

[3]Camargo, H. E., Smith, B. S., Devenport, W. J., and Burdisso, R. A., "Evaluation and Calibration of a Prototype Acoustic Test Section for the Virginia Tech Stability Wind Tunnel," Departments of Aerospace and Ocean Engineering and of Mechanical Engineering, Virginia Polytechnic Institute and State University, Report VPI-AOE-294, Blacksburg, VA, 2005, URL: http://www.aoe.vt.edu/research/facilities/stab/tunnel_acoustics.php.

[4]Smith, B. S., Camargo, H. E., Burdisso, R. A., Devenport, W. J., "Development and Testing of a Novel Acoustic Wind Tunnel Concept," *11th AIAA/CEAS Aeroacoustics Conference*, Monterey, CA, May 23-25, 2005. AIAA-2005-3053

[5]Brooks, T. F., Pope, D. S., and Marcolini, M. A., "Airfoil Self Noise and Prediction," NASA-RP-1218, 1989.

[6]Remillieux, M. C., Camargo, H. E., and Burdisso, R. A., "Calibration of a Microphone Phased-Array for Amplitude in the Virginia Tech Anechoic Wind Tunnel," *NOISE-CON 2007*, Reno, Nevada, October 22-24, 2007.

[7]Barlow, J., Rae, A., and Pope, A., *Low Speed Wind Tunnel Testing*, 3rd edition, Wiley, New York, 1999.